

1 **Determining the depth and upwelling speed of the equatorial Ekman layer from**
2 **surface drifter trajectories**

Deleted: pumping

3
4 Nathan Paldor¹ and Yair De-Leon¹

5
6 ¹Fredy and Nadine Herrmann Institute of Earth Sciences
7 Hebrew University of Jerusalem
8 Edmond J. Safra Campus, Givat Ram, Jerusalem, 9190401 Israel
9

10
11
12
13 Correspondence to: N. Paldor (nathan.paldor@mail.huji.ac.il)
14
15
16
17

18 **Abstract**

19 Trajectories of 500 - 600 drogued surface drifters launched since 1979 in the equatorial ocean are
20 analyzed by employing the results of a new Lagrangian theory of the poleward transport from the
21 equator forced by the prevailing Trade winds. The Lagrangian theory provides an explicit expression for
22 the depth of the Ekman layer that circumvents the application of the 3-Dimensional continuity equation
23 that requires calculating the divergence of horizontal transport, which was the basis of all previous
24 studies on the subject. The analysis is carried out for drifters launched within 1° of the equator that
25 reached final latitude of 3°, 4° or 5° North or South of the equator while remaining in one hemisphere
26 throughout the entire travel time. The analysis yields robust estimates of 45 meters for the Ekman layer's
27 depth and 1.0 meters/day for the upwelling speed of deep water into the layer.

Deleted: Trajectories of more than 500 drogued surface drifters launched since 1979 in the equatorial ocean are analyzed by employing the results of a new Lagrangian theory of wind-driven transport along the equator forced by the prevailing Trade winds. The analysis yields robust estimates of 45 meters for the Ekman layer's depth and 1.0 meters/day for the upwelling speed of deep water into the layer.

1. Introduction

The Trade winds that blow westward in the Tropics as part of the Hadley circulation are the first and basic component of the heat transport from the warm equatorial surface ocean to the cold poles that mitigates the overall pole-to-equator temperature gradient on Earth. The mechanism that enables the poleward time-independent heat transport is the surface flow in the ocean that is directed 90° to the right/left of the wind in the northern/southern hemisphere relative to the direction of the overlying wind. This counter-intuitive flow direction results from Earth's rotation that adds the Coriolis force to the stress applied by the winds at the ocean surface. This straightforward scenario of wind-driven ocean circulation appears in all textbooks (Knauss, 1996; Talley et al., 2011) but despite its convincing simplicity, currently, quantitative estimates of the parameters that control it vary widely depending on the data and method used in the calculations of these estimates.

The classical theory that describes the ocean response to forcing by the overlying winds was developed about 120 years ago by V.W. Ekman under the assumption of constant Coriolis frequency (Ekman, 1905). This assumption greatly simplifies the analysis by ensuring that all coefficients in the governing equations are constant. The dynamics described in Ekman's theory includes a steady flow perpendicular to the wind direction and inertial, i.e. force-free, oscillations at the local (constant) Coriolis frequency. This is in sharp contrast to the equatorial region where the Coriolis frequency vanishes at the equator and varies (linearly) with latitude, which turns the equations nonlinear so the oscillation-free flow is not steady as in Ekman's original mid-latitude theory. The poleward directed surface flows in both hemispheres along the equator imply a strong horizontal divergence along the equator which can only be balanced by the upwelling of deeper water into the wind-forced, Ekman, layer. Though the heuristic application of the mid-latitude Ekman theory to the vicinity of the equator is quite straightforward, to-

Deleted: no

Deleted: are available for

62 date, it could not be employed to estimate either the depth of the equatorial Ekman layer or the rate of
63 upwelled volume of water.

Deleted: the heuristic application

64 The complications that result from the inclusion of the meridional variation of the Coriolis frequency in
65 Ekman's theory were recently resolved in a theory of wind-driven flow in which Ekman's 1905 classical
66 theory was extended to the equatorial region (Paldor, 2024). This new theory employs the adiabaticity
67 method (Goldstein, 1980; Paldor and Friedland, 2023) that filters out fast oscillatory dynamics from the
68 slow dynamics associated with the motion of the center of oscillation. The application of this general
69 method to the equatorial Ekman problem filters out the oscillation that result from the meridionally
70 varying Coriolis force from the slow and monotonic poleward motion of a water column forced by the
71 combination of the wind stress and the Coriolis force. The essence of the method is the formulation of
72 the problem as the dynamics of a (quasi-)particle about the minimum of a potential while the potential
73 itself varies with time on a slower time scale than the period of oscillations about the minimum. The
74 potential is derived from the meridional Lagrangian momentum equation when the zonal velocity, U , is
75 expressed as $U = D + \int f(y) dy$ where $f(y)$ is the latitude-dependent Coriolis frequency ($= \beta y$) and D is
76 the pseudo angular momentum, which is conserved in the absence of other (body) forces. The
77 substitution of the angular momentum for the zonal velocity is essential for the analysis in spherical
78 coordinates RomKedar et al. (1997). Additional details of the theory are given in SubSec. 2.1.

Deleted: to

Deleted:

Deleted: of a water column under the sole action of the

Deleted:

Deleted: the motion of

79 Direct observations of the depth (thickness) of the equatorial Ekman layer and the rate of upwelling
80 water to it are hard to quantify due to the poor observational definition of the layer's dimensions and the
81 extremely low speed of upwelling. Halpern and Freitag (1987) estimated the upwelling rate in the eastern
82 equatorial Pacific Ocean above 50 m depth to be about 2 m/day from the divergence of several moored
83 horizontal current meters. Below 50 m depth their estimated vertical velocity is negative (directed
84 downward). A similar upwelling rate of 2 m/day extending to depths of 120 m was estimated by Halpern
85 et al. (1989) between 110°W and 140°W from 12/1983 to 9/1984 (but excluding 4/1984) using the same

Deleted: The wind-driven dynamics along the equator can be transformed to this special form only by substituting the pseudo angular momentum for the zonal velocity component in the governing nonlinear equations (Paldor, 2024).

Deleted: not available

method of inferring vertical speeds from the divergence of horizontal currents measured by moored current meters. The upwelling speed decreased eastward in these observations and the variation of the observed values greatly exceeded the mean values. In the same region (Central Pacific) but in 2-3/1980 Bubnov (1989) used a similar observation method of integrating the 3D continuity equation associated with observed horizontal currents, and estimated the upwelling velocity over the upper 300 m to vary between 1 and 8 m/day.

Surface drifter trajectories deployed in the Eastern Pacific during 1977-1982 were used by Hansen and Paul (1987) as proxies of the currents and the trajectory divergence as a proxy of the current's divergence, which resulted in an estimate of 1.5 m/day for the upwelling velocity in a stripe of $\pm 1.5^\circ$ of the equator. For their interpretation they assumed that the drifter trajectories represent the currents and divergence in the top 50 m. As noted by the authors, the main issue with their analysis is the accuracy of representation of currents by drifter trajectories. Using over 700 drifters launched between 1979 and 1990 Poulain (1993) estimated an upwelling velocity of 15 – 20 m/day between 90°W and 150°W in the equatorial Pacific. The method used by Poulain (1993) in the interpretation of drifter observations is to average the drifter velocities in given geographical domains and at selected time intervals to generate the Eulerian velocities at the center of the domain at that time. The high values of upwelling velocity in this study result from the small areas used for inverting the observed Lagrangian drifter velocities to Eulerian fields. Two important conclusions emerge from that study: The first is that except for its western part, the horizontal divergence in the equatorial Pacific is quite uniform and therefore so should be the upwelling speed. The second is that the upwelling velocity decreases monotonically with the assumed width of the meridional band over which the horizontal divergence is calculated.

Estimates of upwelling rates were also calculated based on the distribution of ^{14}C released in large amounts to the atmosphere between 1955 and 1963 when above-ground nuclear tests took place. An analysis of the oceanic uptake of ^{14}C and its redistribution in the Pacific Ocean carried out by Quay et al.

Deleted: In contrast, observations of drifter trajectories are both abundant and accurate so they are used in the present study to estimate these important features of the equatorial Ekman layer using the new theory of wind-driven transport in the equatorial ocean.

(1983) yielded an estimate of about 0.3 m/day for the upwelling velocity along the equator. Aside from this geo-isotopic study the previous estimations of the horizontal divergence fields were estimated either directly from current meter observations or indirectly from drifter trajectories. In the latter case that data were either spatially averaged to yield the Eulerian fields or interpreted as proxies of these fields. In contrast, the current study applies a recently developed Lagrangian dynamical theory directly to observed drifter trajectories which bypasses the need to estimate first the horizontal divergence. The large number of drifters, the accurate tracking of their location by satellites and the longtime of coverage allows for a selection of sufficient number of drifter trajectories that satisfy pre-determined selection criteria and yields accurate estimates of the depth of the equatorial Ekman layer and the speed of upwelling into it.

The application of the Lagrangian theory to drifter observations and the data used in this study are detailed in Section 2. In Section 3 we give the results obtained by applying the theory to drifter trajectories and the study is summarized in Section 4.

2. Theory and Data

2.1. Theory

The recent extension of the wind-driven theory of ocean circulation to the equator described in Paldor (2024) has demonstrated that, as in Ekman’s original theory, the oceanic response can be decomposed into a monotonic, slow, flow (which is directed poleward in the equatorial region) and fast, large amplitude, oscillations. In contrast to Ekman’s original theory, in the equatorial region when the wind stress is directed westward the oscillations are highly nonlinear and of large amplitude. An example of the large amplitude inertial oscillations associated with an initial westward directed velocity when no wind stress affects the motion is shown in Fig. 1a. The present study applies the explicit expressions developed in Paldor (2024) to the observed trajectories of surface drifters and employs the nondimensional variables and parameters in Eq. 10 of Paldor (2024). The dimensional counterpart of this equation is:

- Deleted: (see Fig. 2 of Paldor, 2024)
- Deleted: This new theory
- Deleted: is
- Deleted: d in the
- Deleted: present study
- Deleted: by
- Deleted: considering the dimensional counterpart of the non-dimensional expression derived
- Deleted: 9
- Deleted:
- Deleted: for the oscillation-free latitudinal motion of a water column or drifter launched near the equator:

162
$$\frac{dy}{dt} = \frac{1}{y(t)} \frac{-\tau^x}{H} \left(\frac{R_e}{2\Omega\rho} \right). \quad (1)$$

163 Here, $y(t)$ is the distance from the equator at time t . The global parameters in this relation are: $\rho =$
 164 1027 kg m^{-3} (water density) $\Omega = 7.29 \cdot 10^{-5} \text{ s}^{-1}$ and $R_e = 6371 \cdot 10^3 \text{ m}$ (Earth's rotation frequency
 165 and radius, respectively) so $\left(\frac{R_e}{2\Omega\rho} \right) = 4.25 \cdot 10^7 \text{ m}^4 \text{ s kg}^{-1}$. The remaining, particular, parameters are: τ^x
 166 - the wind stress (units: N m^{-2} ; negative for easterly winds) and H (m) - the Ekman layer's depth.

167 Multiplying the nonlinear relation (1) by $y(t)$ and integrating the resulting 1st order equation for $y(t)^2$
 168 yields:

169
$$y(t)^2 = y(0)^2 + 2 \frac{-\tau^x}{H} \cdot \left(\frac{R_e}{2\Omega\rho} \right) t. \quad (2)$$

170 As demonstrated in Fig. 1b, this expression (shown by the red curve) successfully filters out the inertial
 171 oscillations from the actual latitude time-series (blue curve), and describes the net, oscillation-free, (i.e.
 172 the poleward motion when the inertial oscillations shown Fig. 1a are filtered out) poleward motion.

173 Setting t in Eq. (2) to t_i , the travel time of drifter # i , $y(t)$ to L , a "boundary" of the equatorial region,
 174 and inverting the equation to an explicit expression for H yields the estimate of H based on trajectory # i :

175
$$H = \left(\frac{R_e}{2\Omega\rho} \right) \frac{2(-\tau^x)}{L^2 - y_i(0)^2} t_i, \quad (3)$$

176 where $y_i(0)$ is the distance of drifter # i from the equator at $t = 0$ (i.e. the distance of the launch point
 177 from the equator). The values of H are calculated from this equation for each drifter and then averaged
 178 to yield the mean value for the particular value of L .

179 2.2. Drifter trajectories

180 Nearly 30,000 surface drifters were released from 1979 at the ocean surface (Lumpkin et al., 2017) and
 181 the geographical trajectories of these drifters are tracked by satellites every 6 hours for periods of up to

- Deleted:** (2)
- Deleted:** can be
- Deleted:** applied to
- Formatted:** Font: Italic, Complex Script Font: Italic
- Deleted:** observations of drifter
- Deleted:** ies
- Deleted:** by inverting it to the following explicit expression for H
- Deleted:** and t_i is its travel time to $L = y(t_i)$, the final distance from the equator

1000 days. These (Lagrangian) observations cover the global ocean and a few percent of them were launched on both sides of the equator in the Pacific, Atlantic and Indian oceans. The slightly negatively buoyant drifter is typically drogued at 15-meter depth, so it provides an estimate of the current in the top 15 meters of the water column where the wind stress is the primary forcing (Lumpkin et al., 2017). The agreement between drifter trajectories and ocean currents demonstrated in Lagerloef et al., (1999) and assumed in Poulain (1993) motivates an analysis of observed drifter trajectories in order to determine the depth of the equatorial Ekman layer and the upwelling speed of deep water into it.

Deleted: the
Deleted: of surface drifters

The drifter trajectories used in the analysis are freely available from NOAA Global Drifter Program (NOAA/AOML/GDP) site. The data were screened according to the following three criteria:

Deleted: were collected and made
Deleted: by
Deleted: the

1. They were launched within $1^\circ \approx 110$ km south or north of the equator (regarded as the equator).
2. The drifters remained in one hemisphere throughout the entire travel time to the final latitude (equator crossing is not allowed under westward directed wind stress).
3. The drifters were continuously tracked, with gaps no longer than one day, during their motion from the launch point to the final latitude that marks the boundary of the equatorial region (i.e. $3^\circ \approx 330$ km, $4^\circ \approx 440$ km or $5^\circ \approx 550$ km).

The latitudes 3° and 4° were used in previous studies to define the boundaries of the equatorial region (Brady and Bryden, 1987; Lagerloef et al., 1999; Johnson et al., 2001) but in the present study we also used $L = 5^\circ \approx 550$ km to verify the robustness of the calculated averages to the selected values of L .

The case $L = 2^\circ$ is not included in the analysis since the singularity of Eq. (3) at $L^2 = y_i(0)^2$ affects the accuracy of the estimates of H when L is close to $y_i(0)$ i.e. for $L = 2^\circ \approx 220$ km (and for $y_i(0) \leq 1^\circ$) the denominator is tiny which can yield extremely high value of H and amplify observational errors.

Moved up [1]: in Eq. (3)
Deleted: For $L = 2^\circ \approx 220$ km the singularity in Eq. (3) at $L^2 \rightarrow y_i(0)^2$ in Eq. (3) yields highly erratic and too high value of H .
Moved (insertion) [1]

Of the ~30,000 drifter trajectories archived in AOML archive as of 8/2024, over 1500 drifters were launched near the equator and reached the final latitude (3° , 4° or 5°) out of which ~700 drifters remained in one hemisphere. The number of drifters in the Atlantic and Pacific oceans that reached each

Deleted: nearly

Deleted: and
Deleted: them
Deleted: about

of the final latitudes is given in the 2nd column of Table 1 that also gives the mean $y_i(0)$ (3rd column) and the mean t_i , (4th column) to the final latitudes (noted in the rows of this table). The Indian Ocean is excluded from the analysis due to the positive mean annual wind stress in it (see Sect. 2.3). No information is available on the fraction of drifters that lost their drogues on their way from $y_i(0)$ to L .

Deleted: includes, in addition

Deleted: ,

Deleted: launch distances of

Deleted: travel times of

Deleted: its

2.3. Wind stress

The daily wind stress values over the oceans, τ^x , used in this work are available at NOAA/CoastWatch site in 0.125° spatial resolution for the period 1999-2009. We calculated the averaged wind stress in the region of the Indian, Atlantic and Pacific oceans in a zonal strip that straddles the equator between $-L$ and $+L$, where L corresponds to 3°, 4° or 5°.

Deleted: These averages are given in the 5th column of Table 1 for the Atlantic and Pacific oceans but not for the Indian ocean where the calculated mean values are positive (so $H < 0$) and small (less than $+0.01 \text{ N m}^{-2}$) probably due to the strong seasonal forcing by the Monsoon system that induces eastward directed zonal winds throughout part of the year in this ocean (Hastenrath and Polzin, 2004; Zhang et al., 2022).

L (degrees)	Number of drifters	Mean $y_i(0)$ (degrees)	Mean t_i (days)	τ^x (Nm^{-2})	Mean H (m)	$W = \frac{H}{t_i} \cdot \frac{L - y_i(0)}{L}$ (m/day)
3.04	610	0.29	29.67	-0.0261	51.10	1.56
4.04	576	0.29	43.43	-0.0264	42.48	0.91
5.04	531	0.29	58.12	-0.027	37.16	0.60

Table 1: Drifter characteristics in the Pacific and Atlantic oceans and the zonal wind stresses there. The shown values of L are larger by a few kilometers compared to the distances corresponding to 3°, 4° or 5° since a drifter is determined to be “at L ” with an offset of up to 6 hours after its passage of that point. Less than 10% percent of the relevant drifters were launched in the Indian ocean which is not included in this table and in the analysis since the annual mean wind stress in the Indian Ocean is directed eastward, which is inconsistent with a poleward directed net motion.

These averages are given in the 5th column of Table 1 for the Atlantic and Pacific oceans, where the values are nearly identical (they differ by no more than a few percentage points) but not for the Indian ocean where the calculated mean values are positive (so $H < 0$) and small (less than $+0.01 \text{ N m}^{-2}$) probably due to the strong seasonal forcing by the Monsoon system that induces eastward directed zonal winds throughout part of the year in this ocean (Hastenrath and Polzin, 2004; Zhang et al., 2022). The decade-

long zonal wind stress observations are considered representative of the climatic values that prevailed throughout the trajectories of all drifters. Though the mean negative values of τ^x in the Atlantic and Pacific Oceans are not uniform (reaching their maximal values in the center of each ocean and tapering off near the continents that bound the ocean on the east and west sides) only the mean values are used.

3. Results

Four representative drifter trajectories are shown in Fig. 2 and they demonstrate the richness of observed trajectories near the equator, the intricate combination of oscillations with slow poleward propagation and the occurrence of equatorial crossing in many trajectories.

Substituting the values of $y_i(0)$ and t_i for each drifter in Eq. (3) and averaging these values over all relevant drifters yields the values of H given in the 6th column of Table 1. The histograms of the H values for each value of L are shown in Fig. 3 so the value of H is best estimates by: $H = 44 \pm 7 \approx 45$ m.

Equation (2) can also be employed to calculate the poleward, oscillation-free, velocity of a drifter on its way from $y_i(0)$ to $L = y(t_i)$ from the drifter's average speed during its travel: $V = \frac{L-y_i(0)}{t_i}$. Thus, the volume divergence (per unit length in x) that results from the anti-parallel, poleward directed, volume fluxes of 2 water columns that are initially conjoined along the equator and move poleward is $2HV = 2H \frac{L-y_i(0)}{t_i}$. The vertical volume flux (per unit length) due to Ekman pumping during t_i is: $2LW$, where W is the pumping speed. Equating the vertical and horizontal fluxes yields $WL = H \frac{L-y_i(0)}{t_i}$ or $W = \frac{H}{t_i} \frac{L-y_i(0)}{L}$. The mean values of H and t_i in Table 1 then yield the mean value of $W \approx 1.0$ m/day for the three values of L .

The estimated H and W values along the equatorial Atlantic and Pacific Oceans are noted in Fig. 4 on a qualitative, textbook, cartoon of the wind forcing and resulting oceanic flow patterns.

4. Summary and Discussion

Deleted: 1

Deleted: 2

Deleted: 3

287 The mean estimates $H = 45 \text{ m}$ and $W = 1 \text{ m/day}$ calculated here based on surface drifter trajectories
288 are more robust compared to prior estimates derived from standard hydrographic observations. Table 1
289 shows that the present estimates of H vary with L by a few meters and those for W by about $0.5 \frac{\text{m}}{\text{day}}$.
290 These variations are smaller than those of estimates based on standard hydrographic data that can vary
291 by a factor of up to 3 (Wyrki, 1981; Brady and Bryden, 1987; Lukas and Lindstrom, 1991; Weingartner
292 and Weisberg, 1991). As an example, the $H = 45 \text{ m}$ value reported here exceeds the estimate of 30-40 m
293 proposed in Lukas and Lindstrom (1991) but the $O(10\%)$ variation of the present estimate is significantly
294 smaller than $O(80\%)$ variation in the latter estimate. In view of the crucial role played by the poleward
295 flow of warm equatorial water in mitigating the large radiative pole-to-equator temperature gradient
296 (Czaja and Marshal, 2006; Hartmann, 2016) a reliable quantification of the initiation of this flow is
297 important for understanding Earth's climate.

298 The zonal stress is not uniform, reaching a maximal value in the center of the Ocean and tapering off
299 towards the boundaries on the east and west. The effect of this variation on the value of H is pronounced
300 in the equatorial Pacific Ocean and calculations of H using the values of τ^x at each drifter's initial location,
301 yield a wider range of H values. These estimates, too, are not exact since the value of τ^x varies along the
302 drifter trajectory. A detailed analysis of the variation of τ^x along a drifter trajectory and its effect on the
303 value of H calculated in that trajectory are left for future work.

304 In contrast to Ekman's theory in mid-latitude, the extension of this theory to the equatorial region
305 implies that the slow net poleward motion of a water column subject to a zonal wind stress must be
306 accompanied by a zonal component. This is a natural results of the inertial oscillation on the equator that
307 involves net zonal translation, whereas in mid-latitudes inertial oscillations are not accompanied by a
308 translatory motion.

309 The results calculated in Sec. 3 focus on the net poleward propagation rate, which neglects the inertial
310 oscillations, while the observed trajectories include both types of motion. The neglect of inertial

oscillations in the observed trajectories is justified based on the fact that the period of these oscillations is much shorter than the temporal length of the averaged trajectory used for calculating H in Eq. (3). The high variability of the geographical trajectories, which is exemplified in Fig. 2, does not permit an estimate of the oscillations' period directly from the trajectories. However, for the values of $\tau = 0.026 \text{ Pa}$ and $H = 45 \text{ m}$ the period of inertial oscillations can be estimated from the scale $T = \left(\beta \cdot \frac{\tau}{\rho H} \right)^{-\frac{1}{3}} \approx 5 \text{ days}$ which is much shorter than the typical 30-60 days trajectory length (see the values of t_i in Table 1). Thus, during the relatively long drifter travel time the poleward motion due to the oscillations averages out to zero, leaving the poleward motion of the oscillations' centers as the sole contributor to the net motion.

The results shown in Table 1 imply a decrease in the value H (and hence the value of W) with the increase in L . Though no explanation is proposed here for this dependence on L this result is consistent with the results reported in Fig. 3 of Poulain (1993), which show that the horizontal divergence decreases monotonically with the width of the latitudinal band. This result is not trivial since Eq. (3) is also satisfied with constant H provided $L^2 \propto t_i$ for $y_i(0) \ll L$. However, the calculated values of t_i for different values L reported in Table 1 only show a power slightly above 1.0 (but significantly smaller than 2.0). The variation of H with L probably originates from a mechanism similar to that depicted in Fig. 4 where the depth of the Ekman layer becomes shallower with the distance from the equator, which affects the $t_i(L)$ relation. We also note that Eulerian calculations of $\frac{\partial v}{\partial y}$ based on spatial averaging of the Lagrangian observations as was done in Poulain (1993) yield an estimate of W/H so additional information is needed for determining each of these parameters (Poulain, 1993 arbitrarily assumed $H = 50 \text{ m}$). In contrast, in the present study H is determined directly from drifter trajectories, which yields an estimate of W based on mass conservation in a box of meridional extend L and depth (thickness) H (and unit zonal length).

The successful application of the new **dynamical** theory of wind-driven equatorial transport in the ocean developed in Paldor (2024) lends credence to the relevance of this theory to observations in the

334 equatorial ocean. This relevance is demonstrated despite the negligence of important factors such as the
335 meridional wind stress (can be significant at short times), the initial drifter velocity (assumed to vanish in
336 the theory) or changes in the zonal wind stress. It can be argued that the calculation and successful
337 application of the oscillation-free speed of poleward wind-driven motion on the equator is of similar
338 significance to ocean dynamics as the development of the expression for the steady transport in the
339 original f -plane Ekman theory.

340

341 **Author contribution:**

342 NP: Initiation of project, writing various drafts and theoretical analysis.

343 YD: Data collection and analysis, editing and production of display items.

344 **Competing interests:** The authors declare that they have no conflict of interest.

345 **Financial support:** The authors happily declare that no funding was received for this study

346 **Data Availability:** The drifter data used in this study are maintained by NOAA/AOML and the
347 wind stress data are maintained by NOAA/CoastWatch, both sites are noted in the list of
348 references

349 **Acknowledgements:** The authors are grateful to two anonymous reviewers whose comments
350 greatly improved the presentation of this paper.

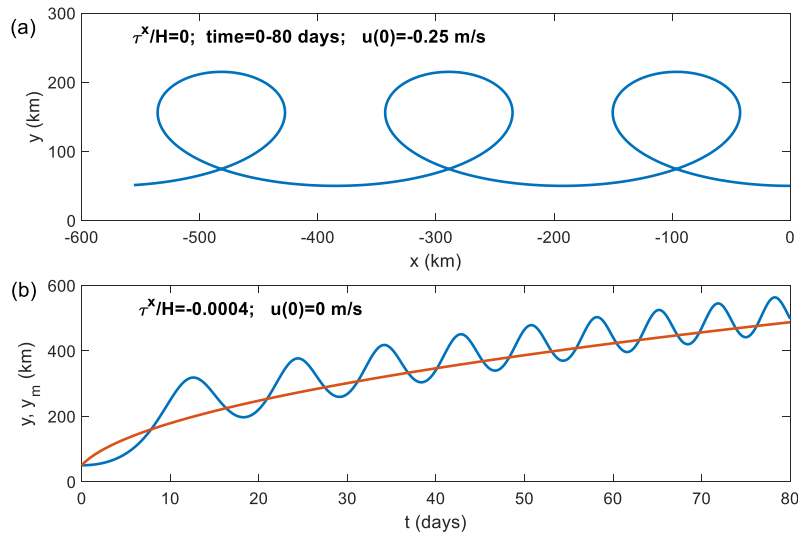


Figure 1: Panel (a): The geographic trajectory of a water column initiated with a westward directed zonal velocity of 0.25 m/s subject only to the, latitude-dependent, Coriolis force. Panel (b): the numerically calculated latitude (i.e. distance from the equator in km) time-series (blue) and the oscillation free latitude time-series given by Eq. (2) denoted here by y_m (red curve) of a 50 m deep water column forced by a westward directed wind stress, τ^x , of 0.02 Pa . In both panels the initial distance from the equator is $y(0)=50 \text{ km}$ while the initial longitude and the initial meridional velocity are both 0 .

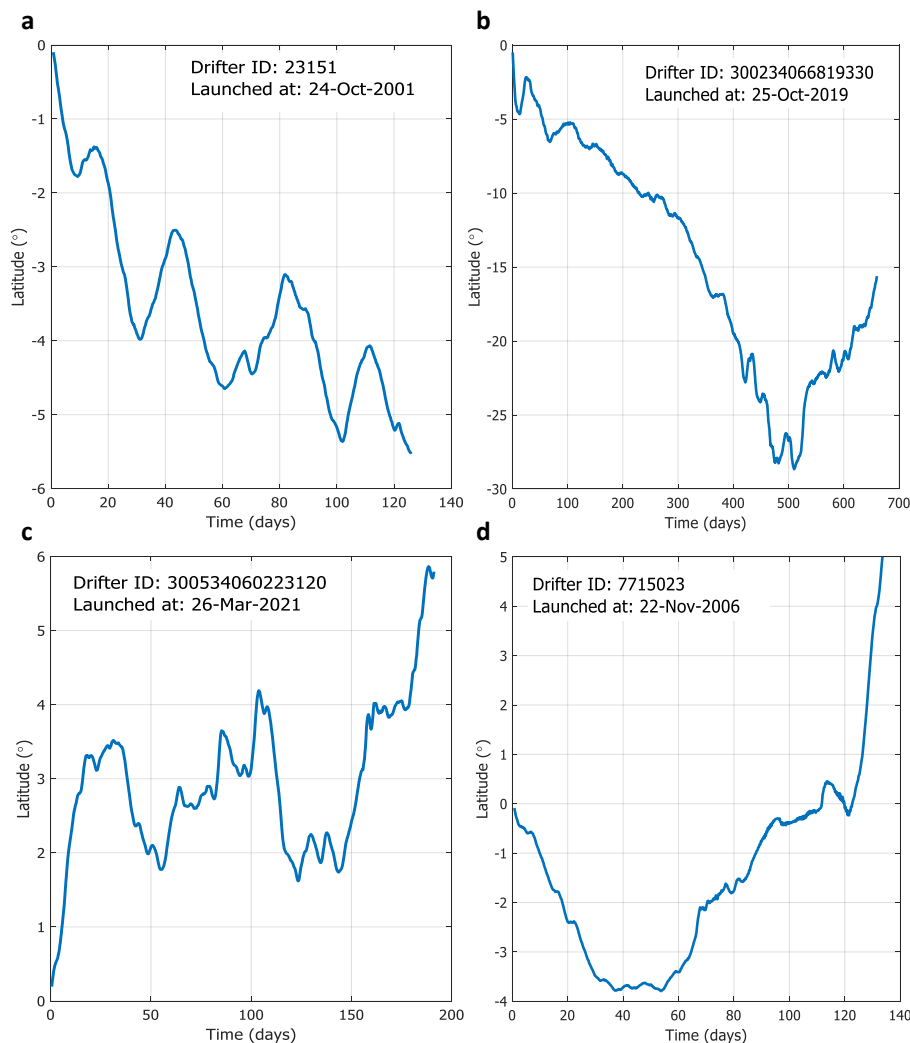


Figure 2: Four drifter trajectories originating within 1° of the equator analyzed in this study. a) A typical southern hemisphere trajectory that clearly shows oscillations and a mean poleward flow; b) A fast southern hemisphere trajectory that reaches 4° in just a few days and remains operational for nearly 2 years; c) A slow northern hemisphere trajectory that reaches 4° in more than 100 days; d) Part of a trajectory that reaches 3° prior to crossing the equator so it is included in the analysis of $L = 3^\circ$ but not in the $L = 4^\circ$ or $L = 5^\circ$ analyses since it reaches these latitudes only after crossing the equator.

Formatted: Left, Line spacing: single

Deleted: 1

Deleted: northern

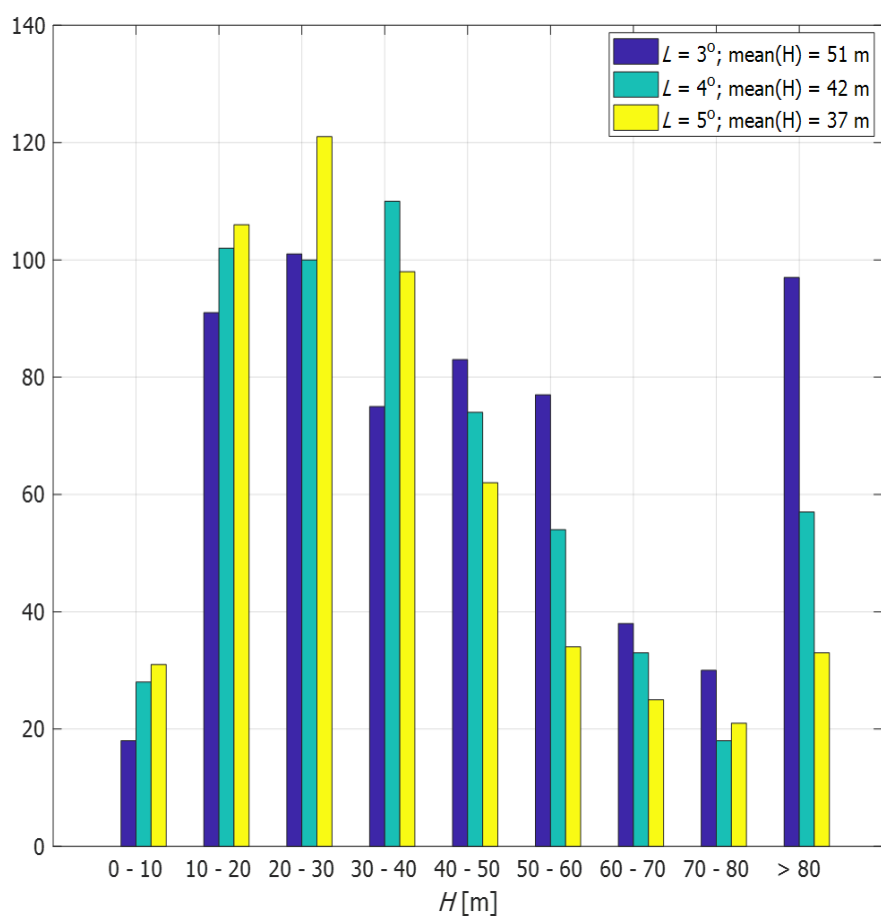
Deleted: A

Deleted: but not 4°

Deleted: cros

Deleted: ses

Deleted: the equator only after reaching 3° N

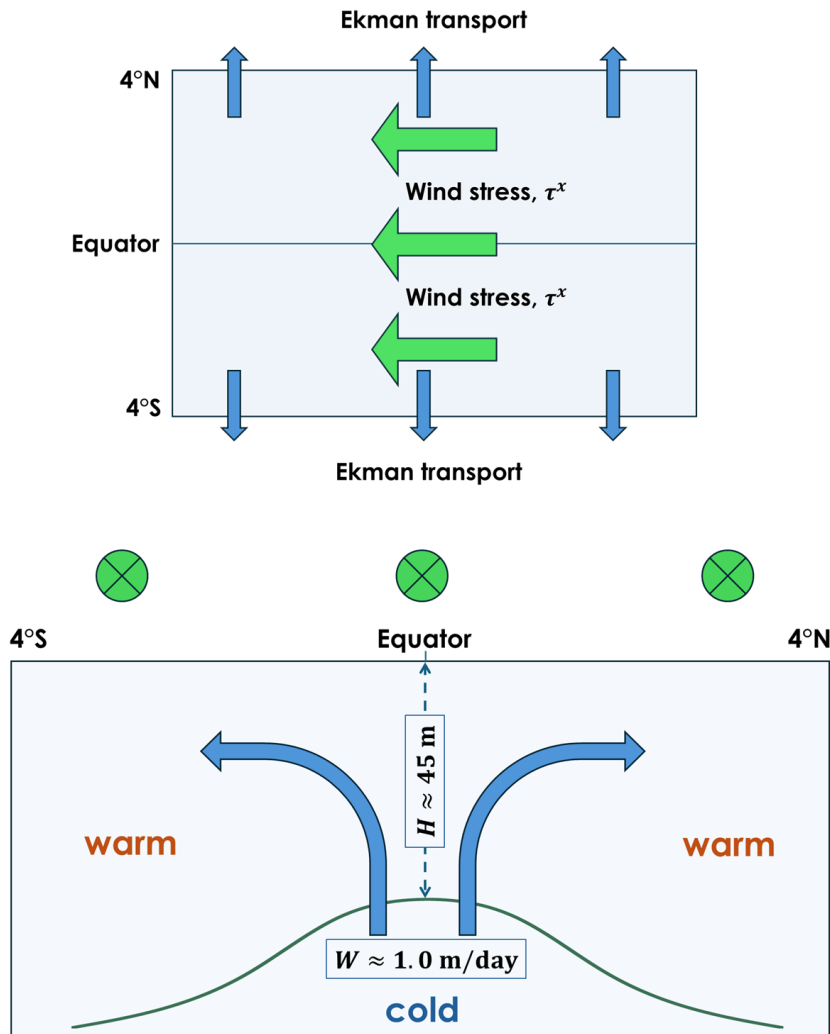


372

373 **Figure 3:** The histograms of H -values for the 3 values of L . For $L = 3^\circ$ the tail of $H > 80$ m is as high as
 374 the maximum cell of $H = 20 - 30$ m consistent with singularity of Eq. (3) at $L = y_i(0)$.

Deleted: L^2

Deleted: $\approx y_i(0)^2$



379 **Figure 4:** A sketch relating the poleward directed wind-driven surface flow along the equator under
 380 westward directed wind stress (upper panel) which is compensated by the upwelling of water from
 381 below (lower panel). The upper panel is a planar view and the lower panel is a latitude-height cross-
 382 section viewed from the east. The $H \approx 45$ m and $W \approx 1.0$ m/day estimates are the main results of
 383 this study.

References

- Bubnov, V. A.: Vertical motion in the Central Equatorial Pacific. *Oceanologica Acta, Special Issue, Gauthier-Villars*. 1987.
- Brady, E. C. and Bryden, H. L.: Estimating vertical velocity on the Equator. *Oceanologica Acta, Special Issue*, 1987.
- Czaja, A. and Marshall, J.: The partitioning of poleward heat transport between the atmosphere and ocean. *J. Atm. Sci.*, **63**(5), 1498-1511. <https://doi.org/10.1175/JAS3695.1>, 2006.
- Ekman, V. W.: On the influence of earth's rotation on ocean-currents. *Ark. Mat. Astr. Fys.*, **2**, 1–52, 1905.
- Goldstein, H.: *Classical Mechanics*. Addison-Wesley, Inc, 1980.
- Halpern, D. and Freitag, H. D.: Vertical motion in the upper ocean of the equatorial Eastern Pacific. *Oceanologica Acta, Special Issue, Gauthier-Villars*. 1987.
- Halpern, D., Knox, R. A., Luther, D. S. and Philander, S. G. H.: estimates of equatorial upwelling between 140° and 110°W during 1984. *J. Geophys. Res.:Oceans*. **94**(C6), 8018-8020. <https://doi.org/10.1029/JC094iC06p08018>. 1989
- Hansen, D. V. and Paul, C. A.: vertical motion in the Eastern equatorial Pacific inferred from drifting buoys. *Oceanologica Acta, Special Issue, Gauthier-Villars*. 1987.
- Hartmann, D. L.: *Global Physical Climatology*, 2nd Ed., Elsevier Inc. <https://doi.org/10.1016/C2009-0-00030-0>. 2016.
- Hastenrath, S. and Polzin, D.: Dynamics of the surface win field over the equatorial Indian Ocean. *Q. J. R. Meteorol. Soc.*, **130**. 503-517. <https://doi.org/10.1256/qj.03.79>, 2004.
- Johnson, G. C., McPhaden, M. J., and Firing, E.: Equatorial Pacific Ocean Horizontal Velocity, Divergence, and upwelling. *J. Phys. Oceanogr.*, **31**(3), 839-849. [https://doi.org/10.1175/1520-0485\(2001\)031<0839:EPOHVD>2.0.CO;2](https://doi.org/10.1175/1520-0485(2001)031<0839:EPOHVD>2.0.CO;2), 2001.
- Knauss, J. A.: *Introduction to Physical Oceanography*, 2nd Ed. Prentice Hall, Inc. ISBN 0-13-238155-9, 1996.
- Lagerloef, G. S. E., Mitchum, G. T., Lukas, R. B. and Niiler, P. P.: Tropical Pacific near-surface currents estimated from altimeter, wind, and drifter data. *J. Geophys. Res.: Oceans*, 104(10), 23,313-23,326. <https://doi.org/10.1029/1999JC900197>, 1999.
- Lukas, R. and Lindstrom, E.: The mixed layer of the western equatorial Pacific Ocean *J. Geophys. Res.: Oceans*. **96**, 3343-3357. <https://doi.org/10.1029/90JC01951>, 1991.
- Lumpkin, R., Ozgokmen, T. and Centurioni, L.: Advances in the application of surface drifters. *Ann. Rev. Mar. Sci.*, **9**, <https://doi.org/10.1146/annurev-marine-010816-060641>, 2017.
- NOAA/CoastWatch: <https://coastwatch.pfeg.noaa.gov/erddap/files/erdQSstress3day/erdQStaux3day/>
- NOAA/AOM/GDP: https://erddap.aoml.noaa.gov/gdp/erddap/taledap/drifter_6hour_qc.html
- Paldor, N. and Friedland, L.: Wind-driven transport of the spherical earth. *Phys. Fluids*, **35**, 056604. <https://doi.org/10.5194/os-19-93-2023>, 2023.
- Paldor, N.: A Lagrangian theory of equatorial upwelling. *Phys. Fluids*, **36**, 046605. <https://doi.org/10.1063/5.0202412>, 2024.

422 [Poulain, P.-M.: Estimates of Horizontal Divergence and Vertical Velocity in the Equatorial Pacific. *J. Phys.*](#)
423 [Oceanogr. **23**, 601-607. 1993.](#)

424 [Quay, P. D., Stuiver, M. and Brocker, W. S.: Upwelling rates for the equatorial Pacific Ocean derived from](#)
425 [the bomb 14C distribution. *J. Mar. Res.*, **41**, 769-792. 1983.](#)

426 [RomKedar, V. Dvorkin, Y. and Paldor, N.: Chaotic Hamiltonian Dynamics of particle's motion in the](#)
427 [atmosphere. *Physica. D*, **106**\(3-4\), 389-431. \[https://doi.org/10.1016/S0167-2789\\(97\\)00015-8\]\(https://doi.org/10.1016/S0167-2789\(97\)00015-8\)](#)

428 Talley, L. D., Pickard, G. L., Emery, W. J. and Swift, J. H.: *Descriptive Physical Oceanography: An*
429 *Introduction*, 6th Ed. Academic Press. ISBN: 978-0-7506-4552-2, 2011.

430 Weingartner, T. J. and Weisberg, R. H.: On the annual cycle of equatorial upwelling in the central Atlantic
431 Ocean, *J. Phys. Oceanogr.*, **21**(1), 68-82. [https://doi.org/10.1175/1520-](https://doi.org/10.1175/1520-0485(1991)021<0068:OTACOE>2.0.CO;2)
432 [0485\(1991\)021<0068:OTACOE>2.0.CO;2](https://doi.org/10.1175/1520-0485(1991)021<0068:OTACOE>2.0.CO;2), 1991.

433 Wyrski, K.: An estimate of equatorial upwelling in the Pacific. *J. Phys. Oceanogr.* 11(9). 1205-1214.
434 [https://doi.org/10.1175/1520-0485\(1981\)011<1205:AEOEUI>2.0.CO;2](https://doi.org/10.1175/1520-0485(1981)011<1205:AEOEUI>2.0.CO;2), 1981.

435 Zhang, L., Li, Y. and Li, J.: Impact of equatorial wind stress on Ekman transport during the mature phase of
436 the Indian Ocean Dipole. *Clim. Dyn.* **59**, 1253–1264. <https://doi.org/10.1007/s00382-022-06183-7>,
437 2022.